

# Overexpression of a pear B-class MADS-box gene in tomato causes male sterility

Haiqi Zhang<sup>#</sup>, Wei Han<sup>#</sup>, Tian Linghu, Zhixia Zhao, Azheng Wang, Rui Zhai, Chengquan Yang, Lingfei Xu<sup>\*</sup> and Zhigang Wang<sup>\*</sup>

College of Horticulture, Northwest A&F University, Taicheng Road No. 3, Yangling 712100, Shaanxi Province, China

<sup>#</sup> These authors contributed equally: Haiqi Zhang, Wei Han

<sup>\*</sup> Corresponding authors, E-mail: [lingfxu2013@sina.com](mailto:lingfxu2013@sina.com); [wzhg001@163.com](mailto:wzhg001@163.com)

## Abstract

B-class MADS-box genes are sufficient for the specification of petals and stamens; however, the role of *Tomato MADS-box protein 6 (TM6)* in seed formation in pear remains largely unknown. In this study, *PbTM6a* and *PbTM6b*, characterized as negative regulators of the response to GA<sub>4+7</sub>, were identified as classic B-class MADS-box genes. Additionally, both of the genes encoding proteins carried the highly conserved MADS-box domain, and showed high expression levels in anther, petal and filament of 'Dangshansu'. Overexpression of *PbTM6a* in tomato reduced the number of seeds per fruit. Analysis of the anatomical structure of floral organs revealed that the reduction in seed number in transgenic fruits might be attributed to an obstacle of pollen release due to strongly formed stomium and limited ovary space of ovule development. Moreover, triphenyl tetrazolium chloride (TTC) staining and *in vitro* germination tests of pollen grains indicated that *PbTM6a* overexpression reduced pollen viability and germination rates. Reciprocal crosses showed that the reduction in seed number in transgenic fruits was dominantly caused by the decreased fertility of pollen grains. Subsequent scanning electron microscopy showed that sterile pollen grains were caused by abnormal pollen grains. Additionally, the reduced levels of jasmonic acid (JA), abscisic acid (ABA), indole-3-acetic acid (IAA) and gibberellin A3 (GA3) in transgenic stamens contributed to the development of sterile pollen. Collectively, our results reveal the role of *PbTM6a* genes in controlling male infertility and broaden our understanding of the mechanism underlying the function of B-class MADS-box genes in pear.

**Citation:** Zhang H, Han W, Linghu T, Zhao Z, Wang A, et al. 2023. Overexpression of a pear B-class MADS-box gene in tomato causes male sterility. *Fruit Research* 3:1 <https://doi.org/10.48130/FruRes-2023-0001>

## INTRODUCTION

MADS-box genes regulate diverse aspects of growth and development in flowering plants, including photoperiod response and flowering time control<sup>[1]</sup>, flower meristem determination and floral organ identification<sup>[2]</sup>, pollen fertility regulation<sup>[3]</sup>, seed and fruit development<sup>[4]</sup>, and endocarp development and vegetative development regulation<sup>[5]</sup>. Typically, MADS-box transcription factors are involved in specifying the identity of floral organs, including sepals, petals, stamens, and carpels<sup>[6]</sup>, the genetic formation control of which was deciphered with a genetic model (ABC model) was recently advanced to the ABCDE model<sup>[7]</sup>. Briefly, class A genes including *APETALA1 (AP1)* in *Arabidopsis thaliana*<sup>[8]</sup>, are needed for the formation of sepals. Represented by *AtAPETALA3 (AtAP3)*, *AtPISTILLATAb(AtPI)*, class B plus class A genes determine the development of petals<sup>[9]</sup>. *AtAGAMOUS (AtAG)*, a representative class C gene, functions alone to control the formation of carpels, Class B plus class C genes are required for the identification of stamens<sup>[10]</sup>. Class D genes, such as *AtSEEDSTICK (AtSTK)*, individually regulate the specification of ovules<sup>[11]</sup>, while class E genes represented by *AtSEPALLATA (AtSEP)* genes such as *AtSEP1*, *AtSEP2*, *AtSEP3*, and *AtSEP4*, are necessary for establishing the identity of petals, stamens, and carpels<sup>[12]</sup>.

Different lineages from B-class MADS box genes can give rise to distinct phenotypes. *AtAP3* and *AtPI* function as B-class MADS box genes in *Arabidopsis*<sup>[13,14]</sup>, *DEFICIENS (DEF)* and

*GLOBOSA (GLO)* constitute B class MADS box genes function activity in *A. majus*<sup>[15,16]</sup>. Mutations in either one of these genes leads to the transformation of petals into sepals and that of stamens into carpels<sup>[13–18]</sup>. The *AP3* lineage gives rise to two *AP3*-like lineages due to another major duplication at the base of the core eudicots. Two *AP3*-like lineages contain *euAP3* that contains *AP3* itself, and *TM6*, which lacks a representative in *A. thaliana*<sup>[19,20]</sup>. Silencing *Tomato AP3 (TAP3)* in the tomato ovary using a specific promoter resulted in male sterility and parthenocarpy<sup>[21]</sup>. In consideration of the differences between siliques in *Arabidopsis* and pome fruit derived from both ovary and hypanthium tissues in apple (*Malus domestica*), silencing of the *MdPI* gene confers parthenocarpy and results in the transformation of petals into sepals and of stamens into pistils, respectively<sup>[22,23]</sup>. In the *parthenocarpic fruit (pat)* mutant of tomato, autonomous development of ovary is associated with the altered expression of class B MADS box genes, including *stamenless (sl)*, *pistillate (pi)* and *SIDEFICIENS (DEF)*<sup>[24]</sup>. Different from the phenotype of mutation in *TAP3*, RNA interference (RNAi)-induced reduction in *TM6* expression results in different phenotypes with homeotic defects primarily in stamens and normal carpel tissue in appearance<sup>[25]</sup>. Tomato male sterility may be a consequence of reduced expression of *SITM6*<sup>[26]</sup>. Overexpression of *TM6* can partially restore the *tap3* second whorl phenotype, but *TAP3* and *TM6* showed different expression patterns and distinct functions in flower development<sup>[25]</sup>.

Different lineages from class B MADS-box genes have complex biological functions during flower development, these orthologues in pear remain largely unrevealed.

Ectopic expression is sufficient for the identification of classic B function. Ectopic expression of *AtAP3* results in the conversion of carpels into stamens, and fails to form a functional gynoecium, resulting in a female sterile flower<sup>[13]</sup>. Flowers of plants ectopically expressing *AtPI* exhibit different phenotypes, with partial replacement of sepals by petals<sup>[9]</sup>. Plants overexpressing *AtAP3* and *AtPI* together produce flowers containing two outer whorls of petals and inner whorls of stamens and the early flowering and leaf curling<sup>[9]</sup>. Overexpression of *MdPI* results in the complete conversion of sepals into petals and in the production of distinctly flattened fruit as a consequence of restricted cell expansion<sup>[27]</sup>. Despite that, overexpression of *TM6* in wild-type background leads to the production of normal floral identification<sup>[25]</sup>, given that *TM6* has more prominent expression in the stamens and carpels, the function of *TM6* and its roles in fruit development require further understanding.

The down-regulation of *TAP3* leads to parthenocarpic fruit set in tomato<sup>[21]</sup> and the members of B class MADS-box were down-regulated during fruit set<sup>[28]</sup>. Exogenous application of gibberellic acid 4+7 ( $GA_{4+7}$ ) reduced the expression of *PbTM6a* and *PbTM6b* in parthenocarpic pear ovary<sup>[29]</sup>. It compelled us to figure out the function of *PbTM6* on the fruit set process in pear. Silencing *TM6* in *Medicago truncatula*<sup>[30]</sup> or in tomato<sup>[25]</sup> or mutating *FaTM6* in the octoploid Strawberry leads to defects in the anthers and low viability of pollen grains<sup>[31]</sup>. Because of the long breeding cycle and arduous genetic transformation of pear, investigation of the function of candidate genes in this plant species is difficult. Research related to *PbTM6* genes has not been reported in pear to date.

In this study, we explored the potential role of *PbTM6* downstream  $GA_{4+7}$  induced in pear, by generating transgenic tomato lines overexpressing *PbTM6a*. Specifically, we examined the function of *PbTM6a* in fertility, and preliminarily explored the regulatory mechanism underlying its role in male sterility. Our results have shed light on the function of *PbTM6a* in pear, and broaden the function of class B MADS box genes.

## MATERIALS AND METHODS

### Plant materials and growth conditions

Sixteen-year-old 'Dangshansu' pear trees grafted onto *Pyrus betulifolia* Bge rootstocks were used as materials for sampling flowers, which were collected from pear experimental base of Northwest A&F University located in MeiXian County, Shaanxi Province, China (34.28° N, 108.22° E; 562 m). Samples of all treatments were immediately frozen in liquid nitrogen after removal, and stored at -80 °C.

Tomato *Ailsa Craig* (*Solanum lycopersicum* L.), received from Xiangqiang Zhan, from Northwest A&F University, Yangling, China, was used for genetic transformation. Tomato planting conditions: 25 °C during the day, 18 °C at night, and photoperiod 18/6 h.

### Phylogenetic analysis and sequence alignment

The MADS-box proteins from ABCDE model were retrieved from NCBI database ([www.ncbi.nlm.nih.gov](http://www.ncbi.nlm.nih.gov)) and a phylogenetic tree was constructed by the software MEGA X with the Maximum Likelihood method and bootstrap analysis. Boot-

strap values were calculated from 1,000 replicate analyses. The constructive methods were as per our previous study<sup>[32]</sup>. The amino acid sequence alignment of *AtAP3*, *SITM6*, *PbTM6a* and *PbTM6b* was carried out through DNAMAN version 9.

The protein accessions used were as follows: *AtAG* (*Arabidopsis thaliana*, P17839.2); *AtAGL11* (*Arabidopsis thaliana*, Q38836.1); *AtAP1* (*Arabidopsis thaliana*, CAA78909.1); *AtAP3* (*Arabidopsis thaliana*, AAD51902.1); *AtCAL* (*Arabidopsis thaliana*, BAH30315.1); *AtAGL8* (*Arabidopsis thaliana*, Q38876.1); *AtFUL* (*Arabidopsis thaliana*, OAO94650.1); *AtPI* (*Arabidopsis thaliana*, OAO95853.1); *AtSEP1* (*Arabidopsis thaliana*, OAO95853.1); *AtSEP2* (*Arabidopsis thaliana*, OAP07944.1); *AtSHP1* (*Arabidopsis thaliana*, OAP06129.1); *AtSHP2* (*Arabidopsis thaliana*, NP\_565986.1); *MdAG* = *MdMADS15* (*Malus domestica*, NP\_001315863.1)<sup>[33]</sup>; *MdAGL1* = *MdMADS14* (*Malus domestica*, XP\_008342376.1)<sup>[33]</sup>; *MdAGL11* = *MdMADS10* (*Malus domestica*, NP\_001280931.1)<sup>[23]</sup>; *MdAP1* (*Malus domestica*, ACD69426.1); *MdCAL* = *MdMADS2* (*Malus domestica*, XP\_008393256.1)<sup>[34]</sup>; *MdDEF* = *MdMADS23* (*Malus domestica*, XP\_028962429.1; HM122607); *MdSEP1* = *MdMADS8* (*Malus domestica*, NP\_001280893.1)<sup>[35]</sup>; *MdPI* (*Malus domestica*, CAC28022.1); *PbTM6a* (*Pyrus bretschneideri*, XP\_009378222.1); *SIAG* = *TAG1* (*Solanum lycopersicum*, NP\_001266181.1)<sup>[36]</sup>; *SIAGL11* = *TAGL1* (*Solanum lycopersicum*, XP\_004241906.1)<sup>[37]</sup>; *SIDEF*=*TAP3* (*Solanum lycopersicum*, NP\_001234077.2)<sup>[25]</sup>; *SIFUL* (*Solanum lycopersicum*, NP\_001294867.1); *TAP3* (*Solanum lycopersicum*, ABG73412.1)<sup>[25]</sup>; *SIPI* = *TPI* = *SIFBP1* (*Solanum lycopersicum*, NP\_001234075.2; ABG73411.1; XP\_004245202.1)<sup>[25]</sup>; *SIMADS6* = *TM6* = *SITDR6* (*Solanum lycopersicum*, QHB49937.1; ABG48621.1; NP\_001311309.1)<sup>[25]</sup>; *SISEP1* = *TM29* (*Solanum lycopersicum*, NP\_001233911.1)<sup>[38]</sup>; *SITAGL1* (*Solanum lycopersicum*, NP\_001300859.1); *SIAGL6* (*Solanum lycopersicum*, NP\_001348459.1); *VvAGL11* = *VvMADS5* = *VvAG3* = (*Vitis vinifera*, QSX80212.1; AOA217EJJO.1); *VvAP3* = *VvAP3a* = *VvPMADS1* = *VvDEF* (*Vitis vinifera*, EOCPH4.1; RVW50380.1)<sup>[39]</sup>; *VvMADS2* (*Vitis vinifera*, XP\_019080194.1); *VvMADS1* = *VvAGAMOUS*/*SHATTERPROOF* (*Vitis vinifera*, NP\_001268105.1)<sup>[40]</sup>; *VvAG* (*VvAGAMOUS*) = *AG1* or *AG2* (*Vitis vinifera*, NP\_001268097.1)<sup>[41]</sup>; *AnDEFA* (*Antirrhinum majus*, P23706.1); *AnGLO* (*Antirrhinum majus*, Q03378.1).

### Tissue-specific expression analysis

*PbTM6a* and *PbTM6b* specific quantitative primers were designed by their reference sequence on the NCBI website ([www.ncbi.nlm.nih.gov](http://www.ncbi.nlm.nih.gov)) (Supplemental Table S1). The flowers were separated into different floral organs including sepals, hypanthium, petals, filament, anther, style, and ovary of two days before anthesis, anthesis and four days after anthesis and then were used for RNA extraction and subsequently tissue-specific expression analysis. Total RNA extraction and Real-time fluorescent Quantitative Polymerase Chain Reaction (qRT-PCR) was performed as previously described<sup>[42]</sup>. The pear actin- $\beta$  gene was used as an internal standard for expression analysis (Supplemental Table S1).

### Subcellular localization

The CDS of *PbTM6a* after the removal of termination codons was cloned into the pCambia2300 vector fusing with the Green Fluorescent Protein (GFP) reporter under the *Cauliflower mosaic virus* (CaMV) 35S promoter using primers with adaptors (Supplemental Table S2). *Agrobacterium* mediated transient

Overexpressing *PbTM6* leads to male sterility

transformation was used for subcellular localization. *Agrobacterium* containing recombinant plasmid was revitalized twice and suspended with cell resuspension solution (10  $\mu\text{mol}\cdot\text{L}^{-1}$  MES, 10  $\mu\text{mol}\cdot\text{L}^{-1}$   $\text{MgCl}_2$ , 200  $\mu\text{mol}\cdot\text{L}^{-1}$  AS, pH = 5.6), then was transformed into tobacco (*Nicotiana benthamiana*) leaves by injection and the empty vector expressing GFP was used as a positive control. After culture in the dark for 1 d and in the light for 2 d, the back of the tobacco leaf was made into freehand section for GFP observation. The GFP signal was observed with a fluorescence microscope (BX63, OLYMPUS, Japan). Activate and adjust the concentration of the bacterial solution till  $\text{OD}_{600} = 0.6$ , then inject the bacterial solution from the back of the tobacco leaf using a syringe.

**Agrobacterium-mediated tomato genetic transformation**

The full-length *PbTM6a* (LOC103938026) coding sequence (CDs) was isolated from 'Dangshansu' cDNA using primers with adaptors (Supplemental Table S2), and then cloned into the pBI121 vector to generate a recombinant plasmid using a Clone-Express One Step Cloning kit (Vazyme, Nanjing, China), then transformed into *Agrobacterium tumefaciens* strain LBA4404 by heat-shock method. *Agrobacterium* revitalized and suspensions prepared were manufactured following the methods as reported in our lab<sup>[43]</sup>. Tomato genetic transformation was carried out as previously reported<sup>[43]</sup>.

**Paraffin sectioning**

Paraffin sectioning experiments were carried out as previously reported<sup>[29]</sup>. Samples collected were immediately fixed in formaldehyde–acetic acid–alcohol fixative and stored at 4 °C. The samples were dehydrated in ethanol/xylene and embedded in paraffin, sectioned into 8- $\mu\text{m}$ -thick slices, dried, and stained with safranin and fast green. A microscopic imaging system (BX51 + PD72 + IX71, Olympus, Japan) was used to observe the anatomical images.

**Pollen vigor measurement**

TTC (2,3,5-triphenyl tetrazolium chloride) solution was performed to determine pollen grain viability<sup>[44]</sup>. Fresh pollen of wild-type and transgenic tomato were evenly sprinkled on the glass slide, respectively. Dripped with a drop of TTC dye solution, and then covered with a cover glass. Prepared glass slides were observed under an optical microscope after incubating at 37 °C for 15–20 min. The reaction of TTC with succinate dehydrogenase in the mitochondria of living cells yielded red formazan, which are used to indicate cell viability. Living pollen were stained in light red and deeper red. Percentage of pollen viability was calculated by the stained pollen number including light red and deeper red pollen, divided by the total pollen number. Percentage of vigorous pollen was calculated by the deeper stained pollen number divided by the total pollen number.

**Pollen germination test *in vitro***

Pollen germination *in vitro* medium was prepared as follows: 12 g sucrose and 0.03 g Ca ( $\text{NO}_3$ )<sub>2</sub>·4H<sub>2</sub>O, 0.02 g  $\text{MgSO}_4$ ·7H<sub>2</sub>O, 0.01g  $\text{KNO}_3$  and 0.005 g H<sub>3</sub>BO<sub>3</sub> were added to 100 ml ddH<sub>2</sub>O. Agar powder was added to make the final concentration of 0.1% (m/v) after adjusting the pH to 6.5. Next, the medium was heated until the agar completely melted, and then cooled to room temperature. A drop of unset culture medium was added onto the glass slide as the pollen germination bed. The pollen

was evenly sprinkled on the culture bed, cultivated for 1 h under dark conditions at 28 °C. A drop of Sigma-aldrich (0.1%) was added onto the glass slide treated above, then covered with a cover glass. After staining for 5 min, the pollen germination situation was assessed under a fluorescent microscope *in vitro*.

**Reciprocal crosses experiment**

Reciprocal crosses experiment was carried out as previously reported<sup>[45]</sup>. For the female parent, the stamens were removed two days before flowering to prevent self-pollination. Before and after pollination, the inflorescence was bagged for the prevention of natural hybridization. For the male parent, blooming flowers with bright yellow petals, stamens golden, un-scattered pollen were chosen to take anthers and made into pollen. A pencil's rubber-head was used as a pollinator.

**Scanning electron microscope observation of pollen**

Pollens of *PbTM6a*-OE and wild type from the day before flowering was collected and glued to an aluminum sample holder with conductive glue. Scanning electron microscope (S-3400N) was applied for the visualization of pollen morphology. Three visual fields of scanning electron microscope were used for the statistics of normal pollen grain.

**Hormone content determination**

The determination of hormone content was performed as previously described<sup>[46]</sup>. Briefly, tomato stamen samples of wild-type and *PbTM6a*-OE were collected 2 d before anthesis with at least three replicates per treatment. 0.5–1 g of the sample was added into a 2 mL centrifuge tube, and the weight of each sample was recorded for analysis, 1 mL ethyl acetate was used as the extract and added into centrifuge tube, subsequently with vortex and shaken for 10 min, centrifuged at 12,000 rpm for 10 min, and the supernatant was transferred into a new 2 mL tube. The liquid collected was evaporated to dryness with a nitrogen blower, and then dissolved with 200  $\mu\text{L}$  methanol (50%) and filtered through a 0.22- $\mu\text{m}$  filter membrane before testing. The hormones levels were determined by ultra-performance liquid chromatography-tandem mass spectrometry (UPLC-MS/MS) (AB SCIEX Triple TOF 5600+, Darmstadt, IN, USA). UPLC-MS/MS was performed using an ACQUITY UPLC HSS T3 (1.8 mm, Waters, USA) column (2.1 mm  $\times$  100 mm). The specific parameters were as in our previous study<sup>[46]</sup>.

**RESULTS*****PbTM6a* and *PbTM6b*, highly expressed in stamens and petals, were identified as B-class MADS-box genes**

To confirm which class-B MADS box genes the two *PbTM6* genes were orthologues of, phylogenetic analysis of classical MADS box genes were performed. The results showed that both *PbTM6* belong to the B-class MADS box genes and were more closely related to *TM6* than to *TAP3* and *AtAP3* (Fig. 1).

Alignment of the amino acid sequences of *PbTM6a*, *PbTM6b*, *AtAP3* and *TM6* showed that all of these proteins possess a highly conserved MADS domain (1–60 aa) at the N-terminus, and the amino acid sequences of *PbTM6a* and *PbTM6b* were highly similar (Fig. 2a). Expression levels of *PbTM6a* and *PbTM6b* in the flower organs of pear were analyzed by qRT-PCR at developmental stages (2 d before anthesis, at anthesis and 4 d

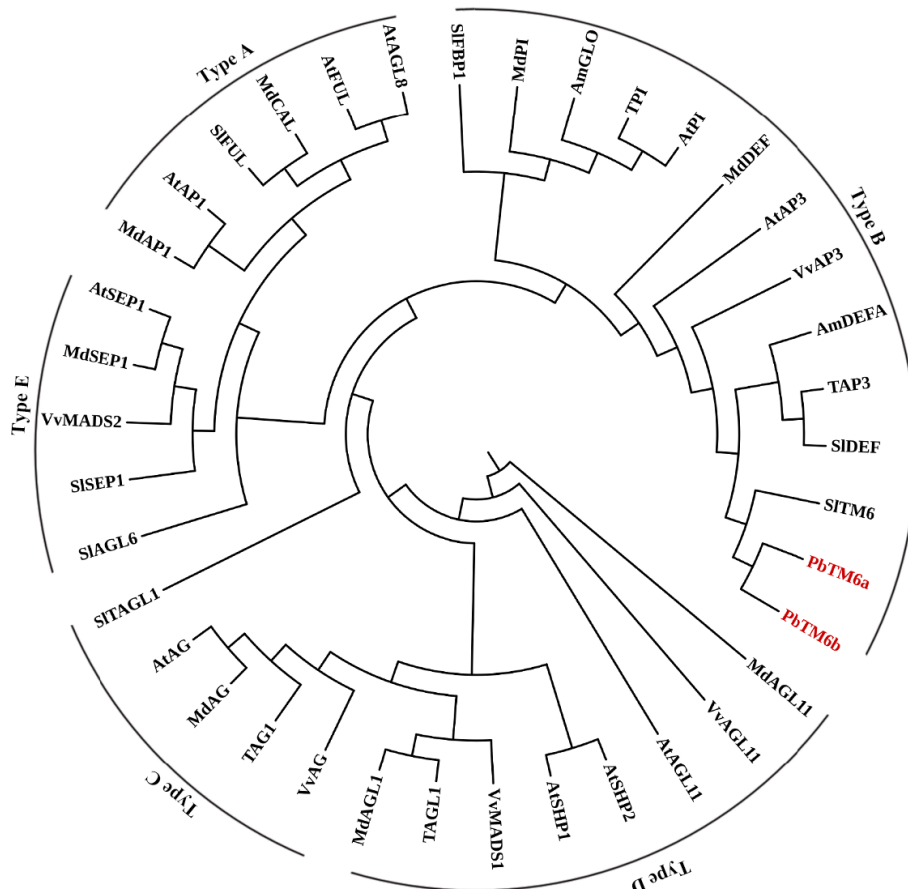


**Fig. 1** Phylogenetic analysis of *PbTM6* and other MADS box proteins involved in the classic ABCDE model.

after anthesis) (Supplemental Fig. S1). The results showed that *PbTM6a* and *PbTM6b* shared similar expression patterns. The expression levels of *PbTM6a* and *PbTM6b* were high in anthers, filaments and petals, which suggested that these genes play important roles in the development of male reproductive organs and petal development (Fig. 2b & c). The expression of *PbTM6a* and *PbTM6b* was down-regulated in pear fruitlets by treatments of  $GA_{4+7}$  (Supplemental Fig. S2). The down-regulation of *PbTM6a* and *PbTM6b* might participate in the pear fruit set process. Subcellular localization analysis via the heterologous expression of a *PbTM6a*-GFP fusion in *Nicotiana benthamiana* leaf epidermal cells showed a fluorescence signal exclusively located in the cell nucleus (Supplemental Fig. S2b), indicating that *PbTM6a* is a nuclear-localized protein. In summary, our results showed that *PbTM6a* and *PbTM6b* correlate with B-class MADS-box genes, and highly expressed in male reproductive organs and petals.

#### Heterologous expression of *PbTM6a* in tomato reduces seed number and size

Since the expression patterns of *PbTM6a* and *PbTM6b* in floral organs and the amino acid sequences of the encoded proteins were highly similar, *PbTM6a* had higher abundance and more significantly decreased expression in parthenocarpic ovaries than *PbTM6b*<sup>[29]</sup>, *PbTM6a* was chosen for further analysis.

To explore the potential function of *PbTM6a* in floral organ identity and fruit development, three *PbTM6a* overexpression (*PbTM6a*-OE) lines were generated in tomato (Supplemental Fig. S3a). It appeared similar between the wild type and

*PbTM6a*-OE lines during the vegetative growth phase. Plant height and growth as leaf size, shape and color of wild-type and *PbTM6a*-OE plants were nearly uniform (Supplemental Fig. S3b). Overexpression of *PbTM6a* seemed to not affect the formation of floral organs compared with the wild type in appearance (Supplemental Fig. S3c). Moreover, flower and fruits of the wild type and *PbTM6a*-OE lines appeared similar during fruit development (Fig. 3a). The number and size of seeds were significantly reduced in the mature fruits of *PbTM6a*-OE lines compared with those of the wild type (Fig. 3b), although the mature fruits of wild-type plant showed traces of retarded seed formation. The statistics of seed number per fruit and seed weight proved the reduced number and size of seeds produced by *PbTM6a*-OE lines (Fig. 3c & d). Thus, we showed that the overexpression of *PbTM6a* in tomato reduces seed size and number.

#### Transgenic tomatoes with overexpression of *PbTM6a* produced anthers and ovaries with subtle changes potentially contributed to reduction in seeds size and number compared to wild type

To explore the cause of the reduction in seed size and number in transgenic tomato, stamens at the late stage of anther development were selected for preparing and analyzing paraffin sections (Fig. 4a). Both transgenic and wild type lines could produce anthers with similar structure and pollen grains (Fig. 4b–g). In addition, the connective tissues between homolateral pollen sacs were broken in wild type, but the stomium bound to the connective tissue appears to be more

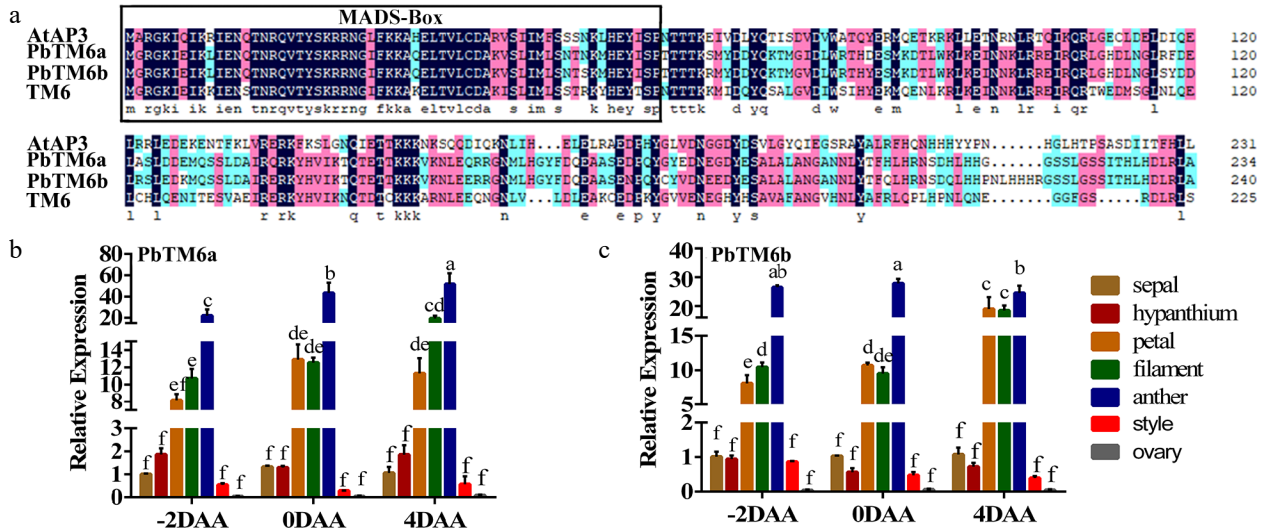


**Fig. 2** (a) Amino acid sequence alignment of *AtAP3*, *PbTM6a*, *PbTM6b*, and *TM6*. MADS-box conserved domains are outlined in black. Expression of (b) *PbTM6a* and (c) *PbTM6b* in different floral organs of pear at different developmental stages. -2 DAA, 2 d before anthesis; 0 DAA, anthesis; 4 DAA, 4 d after anthesis. Data represents mean ( $\pm$  standard deviation (SD)). Significant differences ( $P < 0.05$ ) among treatments are determined by one-way analysis of variance (ANOVA), indicated with different lowercase letters.

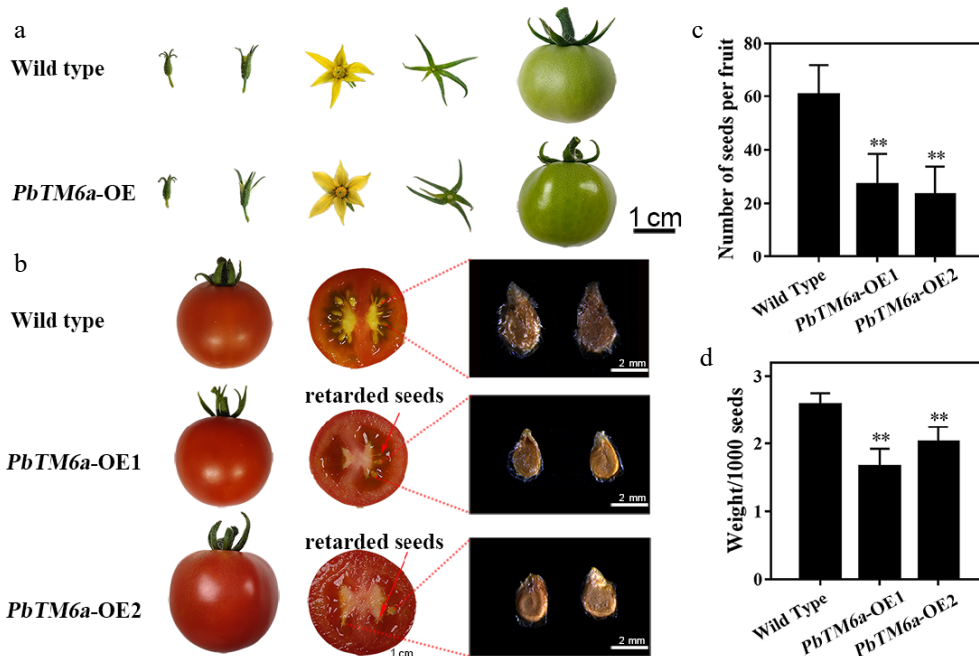


**Fig. 3** Phenotypic analysis of wild type and transgenic tomato plants. (a) Comparison of the growth and development of tomato fruits and the structure of floral organs between the wild type and *PbTM6a* overexpression (*PbTM6a*-OE) lines. (b) Heterologous overexpression of *PbTM6a* decreases the number and size of tomato seeds. (c) Number of wild-type tomato plants and *PbTM6a*-OE lines. (d) Thousand seed weight of wild-type plants and *PbTM6a*-OE lines. Data represents mean ( $\pm$  standard deviation (SD)). Significant differences ( $P < 0.05$ ) among treatments are determined by one-way analysis of variance (ANOVA), indicated with different lowercase letters.

strongly formed in *PbTM6a*-OE anthers, which would influence anther dehiscence.

To confirm whether the reduction in seed number was related to defects in the ovule, the ovary was sampled at anthesis and fruit setting for histological observation. Results showed that the number of maternal ovules seemed similar between *PbTM6a*-OE lines and the wild type (Fig. 4h–k). The total number of ovules in transgenic tomato plants was similar to that in wild type plants even after successful pollination and fertilization (Fig. 4m–o). Moreover, the placenta in transgenic

ovaries was larger than that in wild type and occupied the most space of ovaries which might lead to the arrest of ovules development (Fig. 4h–o). These results indicate that the strongly formed stomium and inflated placenta in transgenic tomatoes might contribute to the reduction in seeds size and number.

**Reduced vigor and germination of *PbTM6a*-OE pollen interfere with successful fertilization**

Because tomato is a self-pollinating crop, defects in pollen germination were speculated as the cause of poor pollination

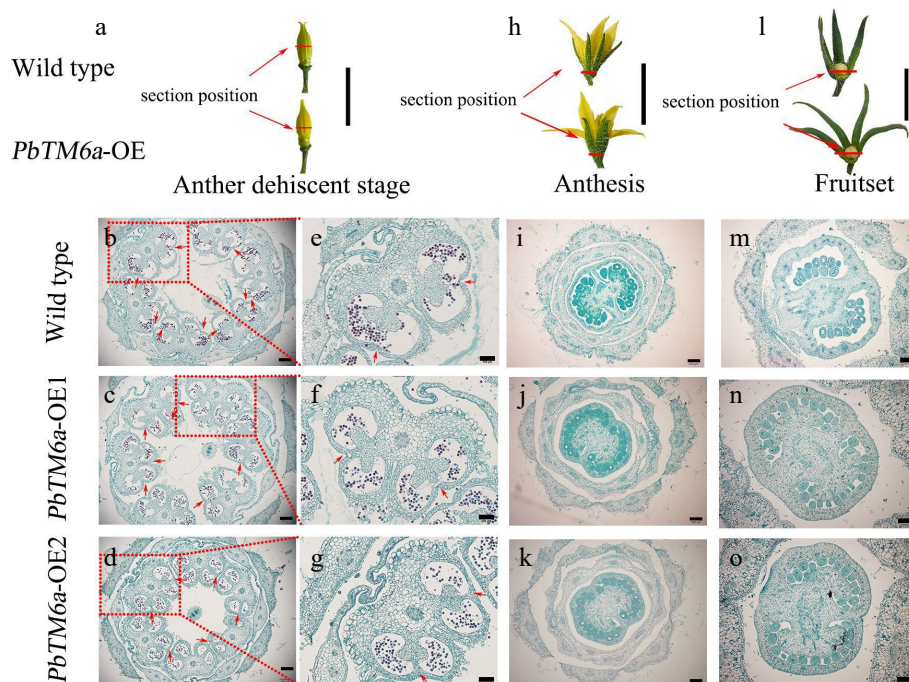


**Fig. 4** Morphological and histological observations of floral organs collected from wild type plants and *PbTM6a*-OE lines. Red lines indicate the section position. (a) Stamens of wild type plants and *PbTM6a*-OE lines after sepals removed at the anther dehiscence stage. (b)–(d) Histological analysis of anthers of the wild type plants and *PbTM6a*-OE lines. (e)–(g) Further analysis of anthers shown in (b)–(d). Arrows indicate the position of stomium. (h) Morphology of wild type and *PbTM6a*-OE flowers at anthesis. (i)–(k) Histological analysis of the cross-section of flowers shown in (h). (l) Analysis of the small tomato fruit of wild-type plants and *PbTM6a*-OE lines after fruit set. (m)–(o) Histological analysis of the cross-section of ovary shown in (l). Scale bars: 2 cm in (a), (h), (l); 200  $\mu$ m in (b), (c), (d), (i), (j), (k), (m), (n), (o); 100  $\mu$ m in (e), (f), (g).

and fertilization. To determine pollen vigor, the pollen of just-opened tomato flowers were selected and used for TTC staining and pollen germination *in vitro*. Pollen with cell viability was stained red. Pollen with no cell viability was not stained. Most of the pollen of wild type plants was stained deep pink with TTC, while most pollen of *PbTM6a*-OE lines stained light pink or did not stain (Fig. 5a–c). The results of pollen germination experiments indicated that the majority of wild-type pollens were capable of germination, whereas only a few transgenic pollens could germinate (Fig. 5d–f). The percentage of fertile pollen was approximately 95% in wild-type plants, which was significantly higher than that in *PbTM6a*-OE1 (8%) and *PbTM6a*-OE2 (11%) lines (Fig. 5g). Similarly, the percentage of vigorous pollen in wild-type plants (81%) was higher than that in *PbTM6a*-OE lines (Fig. 5h). The statistics of germinated pollen supported the results of the germination experiment (Fig. 5i). Overall, our results demonstrated that tomato plants overexpressing *PbTM6a* produced pollen with weak vigor and reduced germination.

To determine whether the reduced seed number and size of *PbTM6a*-OE line were maternally inherited, we carried out reciprocal crosses. Emasculated wild-type tomato plants pollinated with *PbTM6a*-OE pollen produced lower seed number per fruit because of inadequate fertilization; however the seed number was partly restored in transgenic tomato pollinated with wild-type pollen (Fig. 6a). The statistics of seed number coincide with our observation (Fig. 6b, Supplemental Table S3). Therefore, low-vigor pollen produced by *PbTM6a*-OE lines appear to be the dominant factor responsible for unsuccessful fertilization, which in turn led to the production of fruits with less seeds.

#### Low viability of pollen was caused by defective pollen grain development

To determine the cause of the low viability of pollen, we observed pollen morphology by scanning electron microscopy (S-3400N). The pollen grain displayed a smooth and plump surface in wild-type (Fig. 7a), while transgenic pollen showed a sunken surface which was plump in appearance (Fig. 7b, c). Statistics showed that *PbTM6a* overexpressing tomato lines produced much less normal pollen grains compared to that of wild-type (Fig. 7d). Collectively, these findings led us to conclude that *PbTM6a* overexpression in tomato led to defective pollen grains with low vitality and germinating capacity, causing poor pollination and fertilization, which contributed to the formation of fewer seeds per fruit compared with the wild type.

#### Levels of JA, ABA, IAA, and GA3 were reduced in transgenic stamens

Plant hormones were tightly related to pollen development. Therefore, we assessed plant hormone levels in transgenic tomato stamens overexpressing *PbTM6a* (Fig. 8). Remarkably, the content of JA and ABA were reduced in the stamens of *PbTM6a*-OE lines, and the levels of IAA and GA3 were significantly decreased. Thus, we concluded that overexpression of *PbTM6a* in tomato led to the suppression of endogenous JA, ABA, IAA and GA3 levels in stamens, which may be related to male sterility.

## DISCUSSION

Although class-B MADS box genes, especially for *PI* and *AP3*, exhibit a highly conserved function in the formation of petals

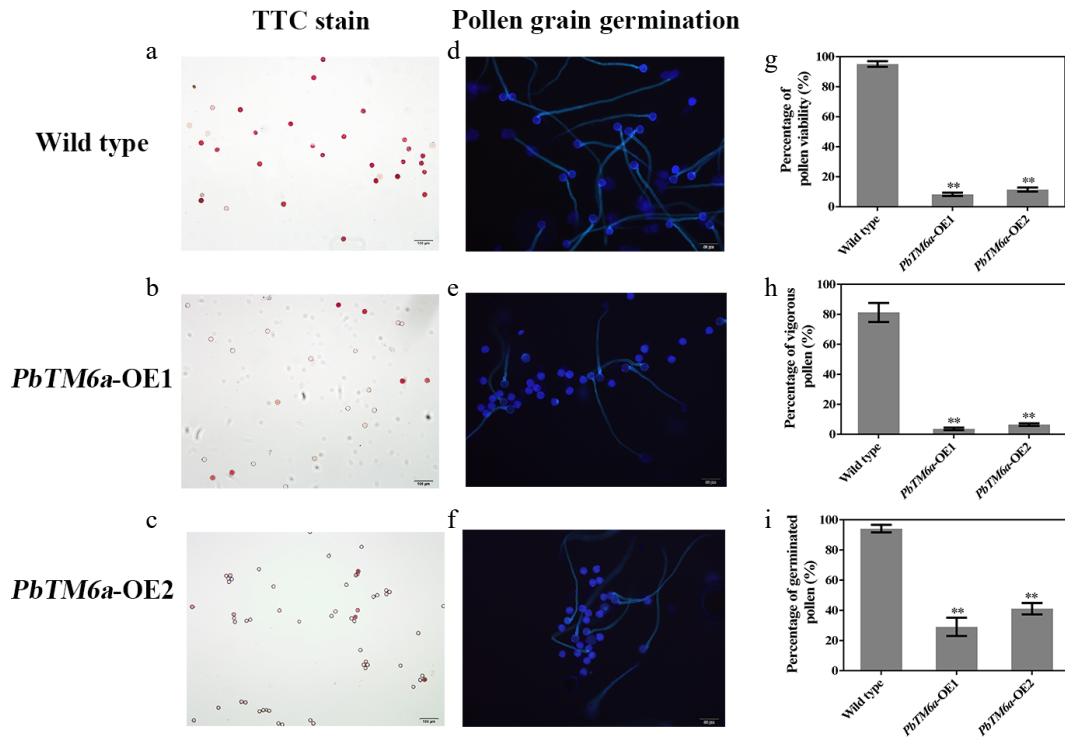


**Fig. 5** Assessment of pollen vigor via the viability evaluated by TTC staining and germination *in vitro*. (a)–(c) Visualization of pollen viability of *PbTM6a*-OE lines and wild-type plants *in vitro* by TTC staining. (d)–(f) Evaluation of *PbTM6a*-OE and wild-type pollen germination *in vitro* under a fluorescence microscope. Statistics of the percentage of (g) pollen viability, (h) vigorous pollen and (i) pollen germination rate (i) in *PbTM6a*-OE lines and wild-type plants. Data represents mean ( $\pm$  standard deviation (SD)). Significant differences ( $P < 0.05$ ) among treatments as determined by one-way analysis of variance (ANOVA), are indicated with different lowercase letters.

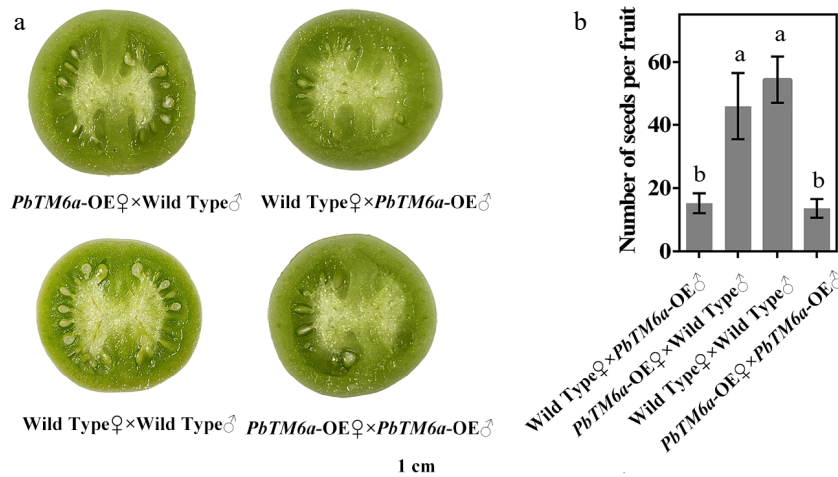


**Fig. 6** Comparison of seed formation and seed number among the progeny of reciprocal crosses and self-pollinations. (a) Seed formation and (b) seed number per fruit produced by *PbTM6a*-OE (♀) × wild Type (♂) and wild Type (♀) × *PbTM6a*-OE (♂) reciprocal crosses and wild-type and *PbTM6a*-OE self-pollinations. Data represents mean ( $\pm$  standard deviation (SD)). Significant differences ( $P < 0.05$ ) among treatments are determined by one-way analysis of variance (ANOVA), indicated with different lowercase letters.

and stamens<sup>[22,25,27]</sup>, mutations in these genes have been reported to cause distinct new phenotypes including parthenocarp, male sterility<sup>[25,26,27]</sup>. Orthologous to AP3, *TM6*, plays a key role in anther development in strawberry<sup>[31]</sup> and tomato<sup>[26]</sup>. However, the role of *TM6* gene in pollen and seed development remains unknown, and research related to *TM6* genes has not yet been reported in pear. Here we identified *PbTM6a* and *PbTM6b* genes from the transcriptome of parthenocarpic ovaries induced by GA<sub>4+7</sub>, and their expression was suppressed

(Supplemental Fig. S1). Here, we reported the response of *PbTM6* genes to GA<sub>4+7</sub> in pear.

Based on phylogenetic analysis of typical members of the ABCDE model<sup>[7]</sup>, *PbTM6a* and *PbTM6b* were classified into class B of the MADS-box gene family (Fig. 1). Like other MADS-box proteins, which contain a highly conserved DNA-binding MADS-box domain of 56–60 amino acids at the N-terminus<sup>[3]</sup>. The *PbTM6a* and *PbTM6b* proteins were also found to possess the conserved DNA-binding MADS-box domain (Fig. 2a). In

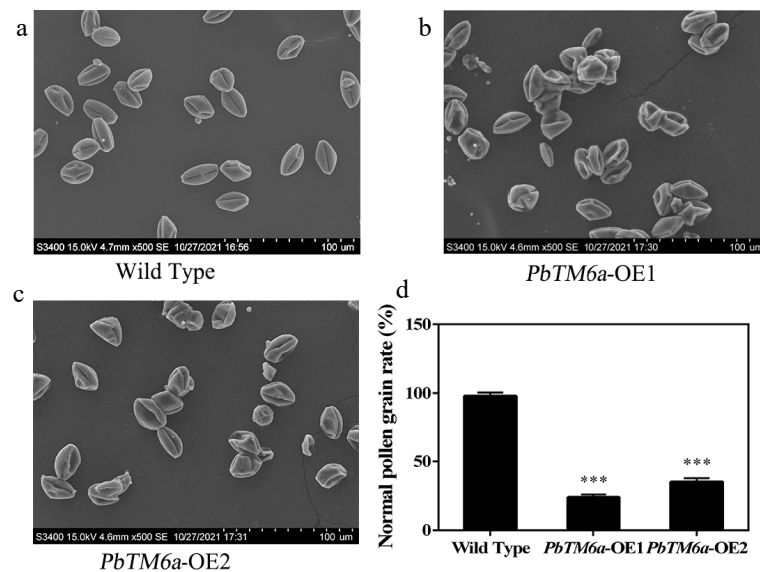


**Fig. 7** Analysis of the morphology of wild-type and *PbTM6a*-OE pollen by scanning electron microscopy. (a) Overview of plump pollen grains of wild type. (b) Overview of plump pollen grains of *PbTM6a*-OE1. (c) Overview of plump pollen grains of *PbTM6a*-OE2. (d) Statistics of the percentage of pollen grain with normal surface in wild-type and *PbTM6a*-OE lines. Data represents mean ( $\pm$  standard deviation (SD) and asterisks represents significant differences ( $P < 0.01$ ) as determined by one-way ANOVA.

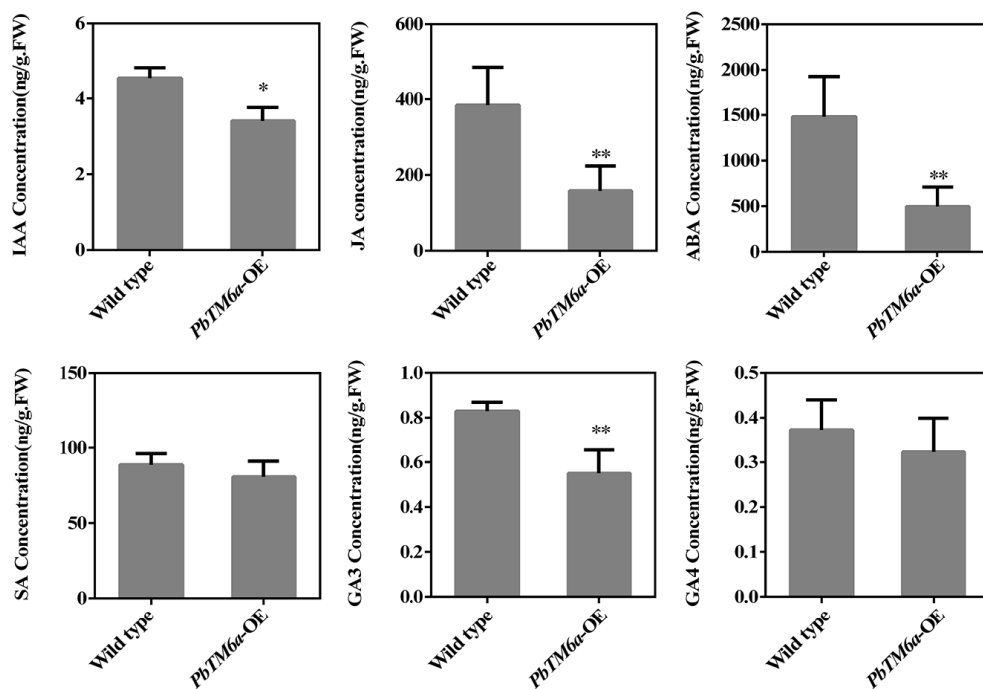


**Fig. 8** Levels of IAA, JA, SA, ABA, SA, GA3, and GA4 in wild-type and *PbTM6a*-OE stamens. Data represents mean ( $\pm$  standard deviation (SD). Asterisks represents significant differences ( $P < 0.05$ ) as determined by one-way ANOVA.

view of the parthenocarpic capacity of *MdPfl*<sup>[22,27]</sup>, repressed expression of *PbTM6a* and *PbTM6b* induced by the GA<sub>4+7</sub> treatment impelled us to determine the involvement of *PbTM6* in floral organ identity. Our results showing higher expression of *PbTM6* in anther, filament and petal were consistent with previous reports, according to which class-B MADS-box genes are highly expressed in stamen and petal<sup>[9,25]</sup>. The *PbTM6a* and *PbTM6b* genes are homoeologues which arose through whole genome duplication. *PbTM6a* had higher abundance and more significantly decreased expression in parthenocarpic ovaries than *PbTM6b*<sup>[29]</sup>, *PbTM6a* was chosen for further analysis.

Because pear has a long breeding cycle and is difficult to transform, tomato was chosen as the heterologous expression system for exploring the role of *PbTM6a* in flowers and fruit development. Mutant in *TM6* mediated by CRISPR/Cas9 system in the octoploid cultivated strawberry leads to distinct petals with modest defects in overall size and color and anthers with a severe reduction in pollen content and viability<sup>[31]</sup>. However, overexpression of *PbTM6a* in tomato did not lead to the conversion of petals and stamens and did not affect the vegetative development of transgenic plants compared with the wild-type (Fig. 3a & Supplemental Fig. S3). Thus, we



Overexpressing *PbTM6* leads to male sterility

speculated that *PbTM6a* has distinctive features compared with classical B-class MADS-box genes such as *AP3* and *PI*.

Surprisingly, the number of seeds per fruit was significantly reduced in *PbTM6a*-OE lines compared with the wild type (Fig. 3b–d). Through histological observations of floral organs, *PbTM6a*-OE lines have more strongly formed stomium bound to the connective tissue in the pollen sac and squeezed ovules in a narrow ovary chamber, which seems to contribute to the reduction in seed number and size (Fig. 4). Further reciprocal crosses and the determination of pollen vigor and germination rate demonstrated that the low vigor pollen produced by *PbTM6a*-OE lines leading to unsuccessful fertilization is the dominant cause for the production of fruits with fewer and smaller seeds (Figs 5–7). Meanwhile the effect of the development of transgenic ovary and ovule itself on the seed formation cannot be excluded in this study. Given that the *PbTM6a* and *PbTM6b* have much lower expression in the ovary compared to petals and anthers (Fig. 2b, c), the development of the ovary and ovule seems not to be the dominant factor affecting seed number and size. Consistent with the speculation, *FaTM6* is not expressed in carpels, carpels of mutants in *FaTM6* shows normal development in octoploid strawberry<sup>[31]</sup>.

Interestingly, *SITM6* has been characterized as a candidate gene for the tomato male sterile-15<sup>26</sup> locus, where the promoter and first four exons of the *TM6* gene were absent<sup>[26]</sup>. The RNAi of *SITM6* resulted in flowers with homeotic defects primarily in stamens<sup>[25]</sup>. It is possible that the heterogenous overexpression of *PbTM6a* leads to post-transcriptional regulation of other endogenous MADS-box genes in tomato. Mutation in *FaTM6* leads to smaller and darker anthers with clear defects in the epidermal cell layer which produce less pollen grain with aberrant and collapsed structure and impaired viability<sup>[31]</sup>. Here ectopic expression of *PbTM6a* can produce abnormal pollen with reduced viability and low germination and sunken surface (Figs 5 & 7). Sophisticated regulation of *TM6* expression is required for pollen development. It demonstrated that *TM6* has a conserved role in the anther and pollen formation.

The integrated regulatory network of JA and other plant hormones participates in male organ development<sup>[47]</sup>. Decreased levels of JA, IAA, ABA and GA3 were detected in the stamens of *PbTM6a* overexpression lines (Fig. 8). In Arabidopsis, the deficiency of JA is tightly associated with male organ development, mutations in genes encoding JA biosynthetic enzymes result in failure of filament elongation, delayed anther dehiscence, and unviable pollen<sup>[48]</sup>. Decreased pollen vigor and germination in *PbTM6a*-OE lines may be a consequence of the decreased JA level. It has been reported that the exogenous application on undehisced anthers can remove the block in pollen release<sup>[49]</sup>. The specific mechanism between *PbTM6a* and genes related to regulating JA content needs to be further demonstrated.

Auxin and its signaling play a key role in male gametogenesis. Two auxin biosynthesis genes, *YUC2* and *YUC6*, exhibit high expression in anther procambium, endothecium, tapetum, tetrads and microspores, and the *yuc2yuc6* double mutant is unable to form viable pollen grains<sup>[50]</sup>. Microsporocyte- or microspore-specific, but not tapetum-specific, overexpression of *YUC2* gene in the *yuc2yuc6* double mutant is sufficient to

rescue abortive pollen formation<sup>[51]</sup>. Similar to the male-sterile phenotype of the JA mutants, the *arf6-2 arf8-3* double mutant produces unviable pollens<sup>[49]</sup>. Male sterility observed in our study could also be a consequence of insufficient IAA content. The production of auxin in anthers is necessary for the advancement of pollen from the microspore stage to the bicellular stage in both Arabidopsis and tomato<sup>[51]</sup>. Auxin seems to act upstream of JA in the development of pollen grains.

A gradual elevation in ABA and IAA levels accompanies the formation of microsporocytes and microspores in the male-fertile lines of petunia (*Petunia hybrida* L.)<sup>[52]</sup>. Ultrahigh levels of ABA and IAA arise in reproductive cells of male-sterile lines. The addition of ABA enhances the viability and reduces the death of barley *Hordeum vulgare* L., which suggests that ABA acts as a potential signal of male sterility<sup>[53]</sup>. Although the involvement of ABA in male sterility lacks direct evidence, accumulating indirect evidence shows that ABA interacts with the sugar signaling pathway<sup>[54]</sup>. Carbohydrates are necessary for sustaining pollen development<sup>[55]</sup>. In tomato, silencing of *Lycopersicon Invertase 5 (LIN5)*, which encodes a cell wall invertase, decreases seed number per fruit and reduces pollen germination and viability<sup>[56]</sup>. The role of ABA in male sterility control needs to be further studied in the future.

In addition, the promotion of bioactive GAs to pollen viability has been determined widely. Bioactive GAs is involved in pollen exine formation and the programmed cell death of tapetal cells in Arabidopsis, rice and tomato<sup>[57]</sup>. Exogenous GA3 application promotes pollen viability and number under cold conditions in almond (*Amygdalus communis* L.)<sup>[58]</sup>. Although the effects of GA<sub>4+7</sub>, when applied to flowers, on pollen germination in pear were not assessed in this study, the expression of *PbTM6a* was repressed by the application of GA<sub>4+7</sub> in pear, confirming that *PbTM6a* acts downstream of GA<sub>4+7</sub> in pear. The low pollen viability production mediated by *PbTM6a* maybe takes in the process of the regulation of GAs to pollen development. Overexpression of *PbTM6a* in tomato showed that low GA level may be the cause of the weak vigor of pollen (Fig. 8).

## CONCLUSIONS

In summary, heterologous overexpression of *PbTM6a* is insufficient for the classical function of class B MADS-box genes in the identification of floral organs, but instead of reduced plant fertility. The specific mitotic progression and the molecular mechanism underlying the role of *PbTM6a* in pollen development should be elucidated in the future. The results of this study provide insight into the conserved role of MADS-box genes in controlling male fertility, and enhance our understanding of the mechanism underlying the function of *PbTM6* in pear.

## ACKNOWLEDGMENTS

This study was supported by the earmarked fund for CARS-28 (China Agriculture Research System).

## Conflict of interest

The authors declare that they have no conflict of interest.

**Supplementary Information** accompanies this paper at (<https://www.maxapress.com/article/doi/10.48130/FruRes-2023-0001>)

## Dates

Received 29 August 2022; Accepted 25 November 2022; Published online 17 January 2023

## REFERENCES

- Zeng X, Liu H, Du H, Wang S, Yang W, et al. 2018. Soybean MADS-box gene *GmAGL1* promotes flowering via the photoperiod pathway. *BMC Genomics* 19:51
- Mandel MA, Yanofsky MF. 1995. A gene triggering flower formation in *Arabidopsis*. *Nature* 377:522–24
- Adamczyk BJ, Fernandez DE. 2009. MIKC\* MADS domain heterodimers are required for pollen maturation and tube growth in *Arabidopsis*. *Plant Physiology* 149:1713–23
- Busi MV, Bustamante C, D'Angelo C, Hidalgo-Cuevas M, Boggio SB, et al. 2003. MADS-box genes expressed during tomato seed and fruit development. *Plant Molecular Biology* 52:801–15
- Dreni L, Zhang D. 2016. Flower development: the evolutionary history and functions of the *AGL6* subfamily MADS-box genes. *Journal of Experimental Botany* 67:1625–38
- Zik M, Irish VF. 2003. Flower development: initiation, differentiation, and diversification. *Annual Review of Cell and Developmental Biology* 19:119–40
- Causier B, Schwarz-Sommer Z, Davies B. 2010. Floral organ identity: 20 years of ABCs. *Seminars In Cell & Developmental Biology* 21:73–79
- Burko Y, Shleizer-Burko S, Yanai O, Shwartz I, Zelnik ID, et al. 2013. A role for *APETALA1/fruitfull* transcription factors in tomato leaf development. *The Plant Cell* 25:2070–83
- Krizek BA, Meyerowitz EM. 1996. The *Arabidopsis* homeotic genes *APETALA3* and *PISTILLATA* are sufficient to provide the B class organ identity function. *Development* 122:11–22
- Theißen G. 2001. Development of floral organ identity: Stories from the MADS house. *Current Opinion in Plant Biology* 4:75–85
- Angenent GC, Franken J, Busscher M, van Dijken A, van Went JL, et al. 1995. A novel class of MADS box genes involved in ovule development in *Petunia*. *The Plant Cell* 7:1569–82
- Melzer R, Verelst W, Theißen G. 2009. The class E floral homeotic protein *SEPALLATA3* is sufficient to loop DNA in 'floral quartet'-like complexes *in vitro*. *Nucleic Acids Research* 37:144–57
- Jack T, Fox GL, Meyerowitz EM. 1994. *Arabidopsis* homeotic gene *APETALA3* ectopic expression: transcriptional and posttranscriptional regulation determine floral organ identity. *Cell* 76:703–16
- Jack T, Brockman LL, Meyerowitz EM. 1992. The homeotic gene *APETALA3* of *Arabidopsis thaliana* encodes a MADS box and is expressed in petals and stamens. *Cell* 68:683–97
- Schwarz-Sommer Z, Hue I, Huijser P, Flor PJ, Hansen R, et al. 1992. Characterization of the *Antirrhinum* floral homeotic MADS-box gene *deficiens*: evidence for DNA binding and autoregulation of its persistent expression throughout flower development. *The EMBO Journal* 11:251–63
- Tröbner W, Ramirez L, Motte P, Hue I, Huijser P, et al. 1992. *GLOBOSA*: a homeotic gene which interacts with *DEFICIENS* in the control of *Antirrhinum* floral organogenesis. *The EMBO Journal* 11:4693–704
- Zahn LM, Leebens-Mack J, DePamphilis CW, Ma H, Theissen G. 2005. To B or Not to B a flower: the role of *DEFICIENS* and *GLOBOSA* orthologs in the evolution of the angiosperms. *Journal of heredity* 96:225–40
- Hernández-Hernández T, Martínez-Castilla LP, Alvarez-Buylla ER. 2007. Functional diversification of B MADS-box homeotic regulators of flower development: Adaptive evolution in protein-protein interaction domains after major gene duplication events. *Molecular Biology and Evolution* 24:465–81
- Kramer EM, Dorit RL, Irish VF. 1998. Molecular evolution of genes controlling petal and stamen development: Duplication and divergence within the *APETALA3* and *PISTILLATA* MADS-box gene lineages. *Genetics* 149:765–83
- Kramer EM, Su HJ, Wu CC, Hu JM. 2006. A simplified explanation for the frameshift mutation that created a novel C-terminal motif in the *APETALA3* gene lineage. *BMC Evolutionary Biology* 6:30
- Okabe Y, Yamaoka T, Ariizumi T, Ushijima K, Kojima M, et al. 2019. Aberrant Stamen Development is Associated with Parthenocarpic Fruit Set Through Up-Regulation of Gibberellin Biosynthesis in Tomato. *Plant and Cell Physiology* 60:38–51
- Tanaka N, Tanaka-Moriya Y, Mimida N, Honda C, Iwanami H, et al. 2016. The analysis of transgenic apples with down-regulated expression of *MdPISTILLATA*. *Plant Biotechnology* 33:395–401
- Yao JL, Dong YH, Morris BAM. 2001. Parthenocarpic apple fruit production conferred by transposon insertion mutations in a MADS-box transcription factor. *PNAS* 98:1306–11
- Mazzucato A, Olimpieri I, Siligato F, Picarella ME, Soressi GP. 2008. Characterization of genes controlling stamen identity and development in a parthenocarpic tomato mutant indicates a role for the *DEFICIENS* ortholog in the control of fruit set. *Physiologia Plantarum* 132:526–37
- de Martino G, Pan I, Emmanuel E, Levy A, Irish VF. 2006. Functional analyses of two tomato *APETALA3* genes demonstrate diversification in their roles in regulating floral development. *The Plant Cell* 18:1833–45
- Cao X, Liu X, Wang X, Yang M, van Giang T, et al. 2019. B-class MADS-box *TM6* is a candidate gene for tomato *male sterile-15<sup>26</sup>*. *Theoretical and Applied Genetics* 132:2125–35
- Yao JL, Xu J, Tomes S, Cui W, Luo Z, et al. 2018. Ectopic expression of the *PISTILLATA* homologous *MdPI* inhibits fruit tissue growth and changes fruit shape in apple. *Plant Direct* 2:e00051
- Zouine M, Maza E, Djari A, Lauvernier M, Frasse P, et al. 2017. TomExpress, a unified tomato RNA-Seq platform for visualization of expression data, clustering and correlation networks. *The Plant Journal* 92:727–35
- Liu L, Wang Z, Liu J, Liu F, Zhai R, et al. 2018. Histological, hormonal and transcriptomic reveal the changes upon gibberellin-induced parthenocarp in pear fruit. *Horticulture Research* 5:1
- Roque E, Serwatowska J, Cruz Rochina M, Wen J, Mysore KS, et al. 2013. Functional specialization of duplicated *AP3-like* genes in *Medicago truncatula*. *The Plant Journal* 73:663–75
- Martin-Pizarro C, Triviño JC, Posé D. 2019. Functional analysis of the *TM6* MADS-box gene in the octoploid strawberry by CRISPR/Cas9-directed mutagenesis. *Journal of Experimental Botany* 70:885–95
- Zhai R, Wang Z, Zhang S, Meng G, Song L, et al. 2016. Two MYB transcription factors regulate flavonoid biosynthesis in pear fruit (*Pyrus bretschneideri* Rehd.). *Journal of Experimental Botany* 67:1275–84
- van der Linden CG, Vosman B, Smulders MJM. 2002. Cloning and characterization of four apple MADS box genes isolated from vegetative tissue. *Journal of Experimental Botany* 53:1025–36
- Suog SK, Yu GH, An G. 1999. Characterization of *MdMADS2*, a member of the *SQUAMOSA* subfamily of genes, in apple. *Plant physiology* 120:969–78
- Wada M, Oshino H, Tanaka N, Mimida N, Moriya-Tanaka Y, et al. 2018. Expression and functional analysis of apple *MdMADS13* on flower and fruit formation. *Plant Biotechnology* 35:207–13
- Pnueli L, Hareven D, Rounsley SD, Yanofsky MF, Lifschitz E. 1994. Isolation of the tomato *AGAMOUS* gene *TAG1* and analysis of its homeotic role in transgenic plants. *The Plant Cell* 6:163–73

Overexpressing *PbTM6* leads to male sterility

37. Vrebalov J, Pan IL, Arroyo AJM, McQuinn R, Chung M, et al. 2009. Fleshy fruit expansion and ripening are regulated by the Tomato *SHATTERPROOF* gene *TAGL1*. *The Plant Cell* 21:3041–62
38. Ampomah-Dwamena C, Morris BA, Sutherland P, Veit B, Yao JL. 2002. Down-regulation of *TM29*, a tomato *SEPALLATA* homolog, causes parthenocarpic fruit development and floral reversion. *Plant Physiology* 130:605–17
39. Poupin MJ, Federici F, Medina C, Matus JT, Timmermann T, et al. 2007. Isolation of the three grape sub-lineages of B-class MADS-box *TM6*, *PISTILLATA* and *APETALA3* genes which are differentially expressed during flower and fruit development. *Gene* 404:10–24
40. Boss PK, Vivier M, Matsumoto S, Dry IB, Thomas MR. 2001. A cDNA from grapevine (*Vitis vinifera* L.), which shows homology to *AGAMOUS* and *SHATTERPROOF*, is not only expressed in flowers but also throughout berry development. *Plant Molecular Biology* 45:541–53
41. Wang Y, Liu Z, Wu J, Hong L, Liang J, et al. 2021. MADS-box protein complex *VvAG2*, *VvSEP3* and *VvAGL11* regulates the formation of ovules in *Vitis vinifera* L. cv. 'Xiangfei'. *Genes* 12:647
42. Cong L, Wu T, Liu H, Wang H, Zhang H, et al. 2020. CPPU may induce gibberellin-independent parthenocarpy associated with *PbRR9* in 'Dangshansu' pear. *Horticulture Research* 7:7
43. Zhang H, Han W, Wang H, Cong L, Zhai R, et al. 2021. Downstream of  $GA_4$ , *PbCYP78A6* participates in regulating cell cycle-related genes and parthenogenesis in pear (*Pyrus bretschneideri* Rehd.). *BMC Plant Biology* 21:292
44. Otero AJ, Rodríguez I, Falero G. 1991. 2,3,5-Triphenyl tetrazolium chloride (TTC) reduction as exponential growth phase marker for mammalian cells in culture and for myeloma hybridization experiments. *Cytotechnology* 6:137–42
45. Tovar-Méndez A, Kumar A, Kondo K, Ashford A, Baek YS, et al. 2014. Restoring pistil-side self-incompatibility factors recapitulates an interspecific reproductive barrier between tomato species. *The Plant Journal* 77:727–36
46. Wang H, Zhang H, Liang F, Cong L, Song L, et al. 2021. *PbEIL1* acts upstream of *PbCysp1* to regulate ovule senescence in seedless pear. *Horticulture Research* 8:59
47. Song S, Qi T, Huang H, Xie D. 2013. Regulation of stamen development by coordinated actions of jasmonate, auxin and gibberellin in Arabidopsis. *Molecular Plant* 6:1065–73
48. Wasternack C. 2007. Jasmonates: an update on biosynthesis, signal transduction and action in plant stress response, growth and development. *Annals of Botany* 100:681–97
49. Nagpal P, Ellis CM, Weber H, Ploense SE, Barkawi LS, et al. 2005. Auxin response factors *ARF6* and *ARF8* promote jasmonic acid production and flower maturation. *Development* 132:4107–18
50. Cecchetti V, Altamura MM, Falasca G, Costantino P, Cardarelli M. 2008. Auxin regulates Arabidopsis anther dehiscence, pollen maturation, and filament elongation. *The Plant Cell* 20:1760–74
51. Yao X, Tian L, Yang J, Zhao Y, Zhu Y, et al. 2018. Auxin production in diploid microsporocytes is necessary and sufficient for early stages of pollen development. *PLoS Genetics* 14:e1007397
52. Kovaleva LV, Voronkov AS, Zakharova EV, Andreev IM. 2018. ABA and IAA control microsporogenesis in *Petunia hybrida* L. *Protoplasma* 255:751–59
53. Wang M, Hoekstra S, van Bergen S, Lamers GEM, Oppedijk BJ, et al. 1999. Apoptosis in developing anthers and the role of ABA in this process during androgenesis in *Hordeum vulgare* L. *Plant Molecular Biology* 39:489–501
54. Eckardt NA. 2002. Abscisic acid biosynthesis gene underscores the complexity of sugar, stress, and hormone interactions. *The Plant Cell* 14:2645–49
55. Chen R, Zhao X, Shao Z, Wei Z, Wang Y, et al. 2007. Rice UDP-glucose pyrophosphorylase1 is essential for pollen callose deposition and its cosuppression results in a new type of thermosensitive genic male sterility. *The Plant Cell* 19:847–61
56. Zanon MI, Osorio S, Nunes-Nesi A, Carrari F, Lohse M, et al. 2009. RNA interference of *LIN5* in tomato confirms its role in controlling brix content, uncovers the influence of sugars on the levels of fruit hormones, and demonstrates the importance of sucrose cleavage for normal fruit development and fertility. *Plant Physiology* 150:1204–18
57. Jacobsen SE, Olszewski NE. 1991. Characterization of the arrest in anther development associated with gibberellin deficiency of the *gib-1* mutant of tomato. *Plant Physiology* 97:409–14
58. Li P, Tian J, Guo C, Luo S, Li J. 2021. Interaction of gibberellin and other hormones in almond anthers: phenotypic and physiological changes and transcriptomic reprogramming. *Horticulture Research* 8:94



Copyright: © 2023 by the author(s). Published by Maximum Academic Press, Fayetteville, GA. This article is an open access article distributed under Creative Commons Attribution License (CC BY 4.0), visit <https://creativecommons.org/licenses/by/4.0/>.